Transient Aerodynamic Characteristics of a Two-Dimensional Airfoil During Stepwise Incidence Variation

Yasuhiko Aihara,* Hisao Koyama,† and Atsushi Murashige‡
University of Tokyo, Tokyo, Japan

The present paper discusses the transient aerodynamic characteristics of a two-dimensional low-speed airfoil whose angle of attack is varied impulsively. The study is mainly an experimental one with observations made of the three dynamic loads, the static pressure distribution, and flow on the airfoil surface, following the airfoil motion. The changes in the characteristics and their aerodynamic causes are investigated in terms of the ultimate angle of attack and the rise time.

Nomenclature

C	= chord length (100 mm)
C_D	= drag coefficient
C_L	= lift coefficient
C_m	= pitching moment coefficient around $c/4$
C_p	= surface static pressure coefficient
$C_{L\max}$	= maximum of C_L in transient state
$C_{L\min}$	= minimum of C_L in transient state
t	= time
tU/c	= nondimensional time
T	= nondimensional rise time (Fig. 2)
$(tU/c)_{C_{L\max}}$	= tU/c from start to attainment of $C_{L\max}$
$(tU/c)_{C_{L\min}}$	= tU/c from start to attainment of $C_{L\min}$
U	= wind velocity (= 3 m/s)
α	= angle of attack
α_s	= static stall angle of attack
τ	= nondimensional time delay between the attainment of specific α and the restoration of static C_L

I. Introduction

In the recent development of aircraft technology, flight at high angle of attack, which has been impossible for conventional aircraft, gives rise to various new difficulties.[1] In flight at high angle of attack, not only the angle of attack but also its rate of change is an important factor. In connection with the motion of a helicopter rotor, for instance, numerous investigations have been made of the transient aerodynamic characteristics of changes in angles of attack higher than stall angle, revealing their unsteadiness, nonlinearity, and hysteresis.[2-6] These transient aerodynamic characteristics are brought about by fluid phenomena such as a change in airstream around the airfoil due to unsteadiness, development and separation of a boundary layer, growth and collapse of vortices, or turbulence, however, their interrelationships are too complicated to be clear. One reason for this complexity apparently lies in the fact that the time constant of the airfoil dynamics and the time constants specific to various fluid phenomena have subtle influences on the phenomena and the transient aerodynamic characteristics. There are numerous studies published dealing with the motions of the unsteady airfoil other than the two-dimensional motion to be discussed in this paper. For instance, Refs. 7-10 deal with the effects of variations in the flow velocity and in the angle of attack. There are other studies[11,12] that have analytically pursued the relationship between dynamic stall and the ambient flowfield. Furthermore, little is known about the effects of Reynolds number, Mach number, airfoil profile, and airfoil motion.[13]

At this stage of information it is natural that the technology should be based on experimentation. In the present paper, instead of a conventional study of an oscillating airfoil, which has been often undertaken, the relations between the transient aerodynamic characteristics of an airfoil with stepwise varied angle of attack and the state of the ambient airflow are experimentally investigated as a basic study leading to application. Another reason for adopting a stepwise varied input is the desirability of obtaining a simple motion for understanding the phenomena in a flow with prominent nonlinearity and hysteresis.

II. Experimental Setup and Procedure

Wind Tunnel

Tests were conducted in a low-speed blowdown wind tunnel with a measuring section 30 cm × 30 cm at the University of Tokyo, Department of Aeronautics, Faculty of Engineering. The wind velocity U was mainly set at 3 m/s and the residual turbulence in the tunnel stream at 0.13%. To maintain the two-dimensionality, parallel side walls were set in the measuring part. Figure 1 shows the experimental system schematically. To suppress development of a boundary layer over the side walls, a 5-mm gap was provided between the nozzle of the wind tunnel and the leading edge of the side wall. It would be difficult to make an analytical prediction of the interference of the wind tunnel walls in such a measuring section. It is well known that in a static test of an airfoil the effective angle of attack usually increases if the measuring section is a closed type, while it decreases if the measuring section is an open type; but in the range of variations in the angle of attack in the present experiment, the influence of the presence of the upper and lower walls on the static characteristics could be so small as to be neglected. In the present study, therefore, considering the predictable vertical fluctuations of the airstream in the unsteady motion, the testing was carried out for a free boundary in the measuring section devoid of the upper and lower walls. Meanwhile the angle of attack was defined as a geometrical angle relative to the airstream axis of the wind tunnel. The side walls were built of transparent acryl resin plates to facilitate the flow visualization.

Received Sept. 27, 1984; revision received April 23, 1985.

*Professor, Department of Aeronautics.
†Research Scientist, Department of Aeronautics.
‡Graduate Student, Department of Aeronautics.

Airfoil

The airfoil was a two-dimensional symmetric airfoil, as illustrated in Fig. 2; a flat plate 10 mm thick with chord length $c = 100$ mm has its leading edge rounded to a radius of 5 mm and its trailing edge tapered with 30 mm of the rear portion formed in two arcs. Along the leading edge and near the trailing edge slits 40 mm and 50 mm in length are provided, which issue kerosene vapor to facilitate the flow visualization. The span is so designed that there is a clearance of 0.5 mm to both side walls of the measuring part. Over the airfoil surface, static pressure holes are provided at chord length positions of 2, 10, 20, 30, 40, 50, 60, 70, and 80%. The static pressure holes measured 0.5 mm in inside diameter and were provided on one side only; accordingly, the angle of attack was changed in inverse direction when the static pressure distributions on the other side were to be investigated. Measurements were done by introducing the static pressure to transducers located outside the wind tunnel (DD-102 manufactured by Toyotakoki, with a diffusion type semiconductor diaphragm). The reference static pressure was a static pressure of the uniform stream, and a linear relationship held between the differential pressure and the output. The frequency response of the transducers was 2 kHz and the measuring system as a whole could follow fluctuations of more than 500 Hz. Such a response characteristic was sufficient for the present experiment.

The angle of attack of the airfoil is made variable around 1/4 chord length position by means of a step motor in accordance with an arbitrary program, one step being 0.9 deg. The rise of α (α ramp) in Fig. 2a is a schematic one, and examples of the temporal change of α in the present experiment are illustrated in Fig. 2b. The time taken for initial acceleration and the time taken for final deceleration were practically identical, and a tendency was recognized that the shorter the time in which the angle of attack increased, the less linear became the change. The mechanical vibration accompanying a change in the angle of attack of the airfoil in the absence of the airstream was investigated using a three-component balance. This vibration, which had a sufficiently higher frequency than an aerodynamic change, was deducted in the course of data processing. The changes in lift, drag, and pitching moment could be measured by a three-component measuring balance of strain gage type attached to the rotating shaft. When the airfoil was attached to the balance (load cell LMC-3013 manufactured by Nissho Electric Works), the frequency response characteristic could be verified up to more than 1 kHz in the results of dynamic test.

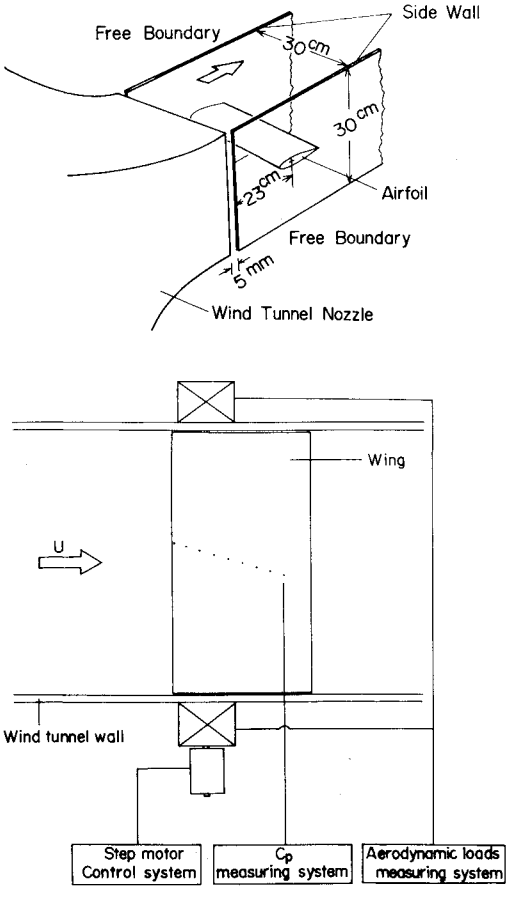

Fig. 1 Schematic diagram of experiment.

Data Processing

The output of the instrument was registered on magnetic tape and processed in an electronic computer. Reproducibility of the data obtained was extremely good.

III. Results and Discussion

The results obtained from tests with Reynolds number set at 2×10^4 are as follows. (Figure 3 illustrates the static characteristics of the airfoil.) The lift coefficient C_L increases linearly up to an angle of attack $\alpha = 9.0$ deg and thereafter exhibits a stall of mixed type. The drag coefficient C_D reaches a maximum at $\alpha = 12.5$ deg, thereafter dropping somewhat but again increasing with α. The pitching moment coefficient C_m

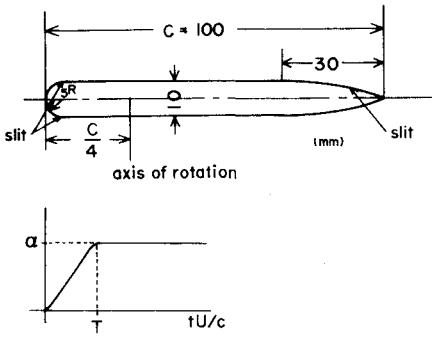

Fig. 2a Two-dimensional symmetric airfoil.

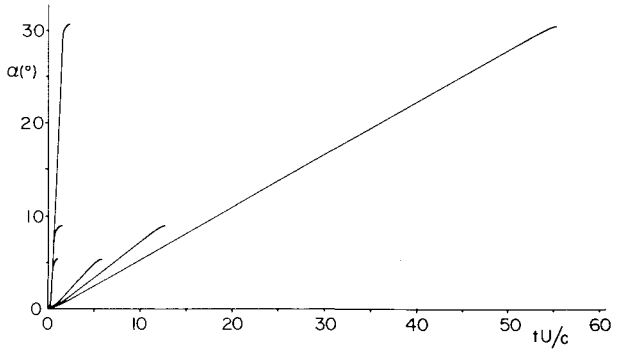

Fig. 2b Temporal change of α.

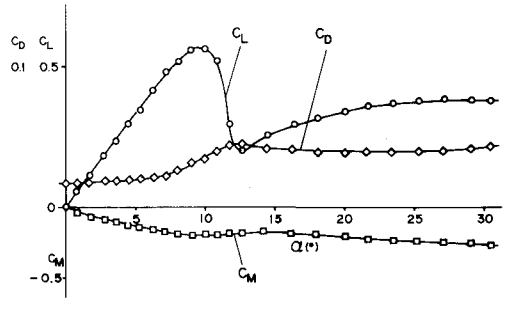

Fig. 3 Static characteristics of the airfoil.

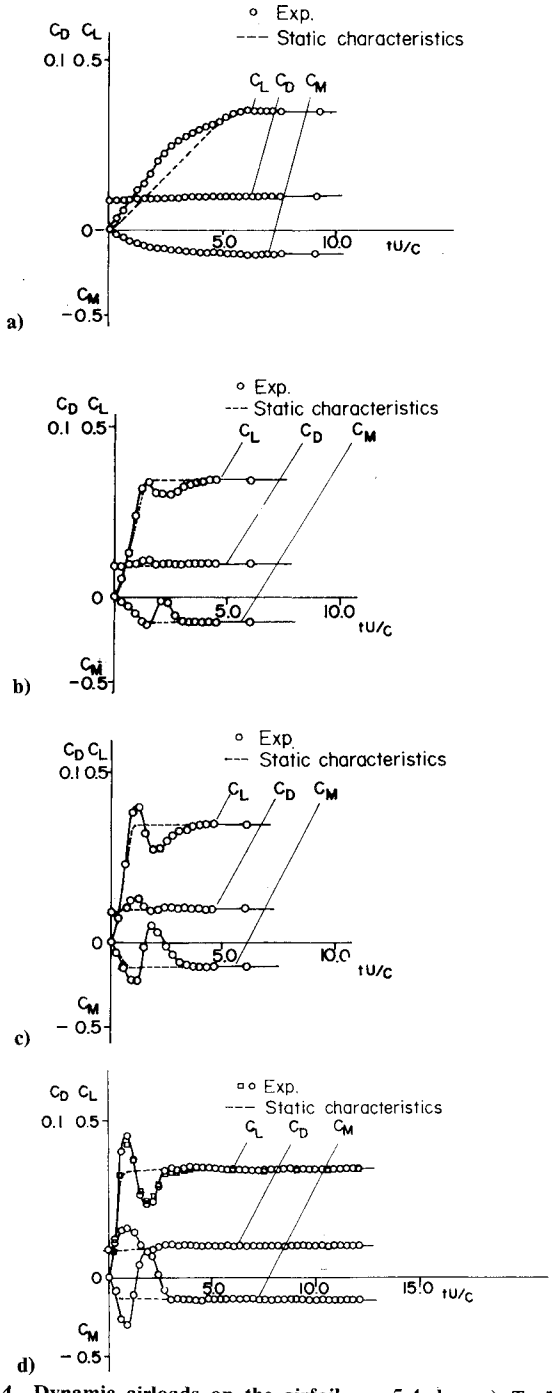

Fig. 4 Dynamic airloads on the airfoil. $\alpha = 5.4$ deg. a) $T = 5.79$, b) $T = 1.57$, c) $T = 1.09$, and d) $T = 0.84$.

around $c/4$ maintains a stable nose-down characteristic up to $\alpha = 30$ deg.

The transient aerodynamic characteristics to be discussed are three typical values of α. Time t is expressed nondimensionally as tU/c, with the starting point of change from $\alpha = 0$ put as zero. The nondimensional rise time is put as T (Fig. 2).

$\alpha = 5.4$ deg

While the value of α is sufficiently lower than the static stall angle α_s, the effect of boundary-layer separation in the range of T of the present test is not significant. Figure 4 illustrates the temporal change in the aerodynamic characteristics. When T is long, condition a, C_L is higher at midpoint than the static value (broken line), but in general it may be called quasi-steady. To have $\tau = 0$ under condition a we put a nondimensionalized time delay before the static characteristic of the relevant C_L is restored by the airfoil after it has attained a specified value of α. As T becomes shorter, the deviation from the static characteristic enlarges and the value of τ increases. Thus, C_L exhibits a peak $C_{L\max}$ higher than the one statically obtained, followed by $C_{L\min}$ lower than the static value; and the static characteristic is restored with a time delay.

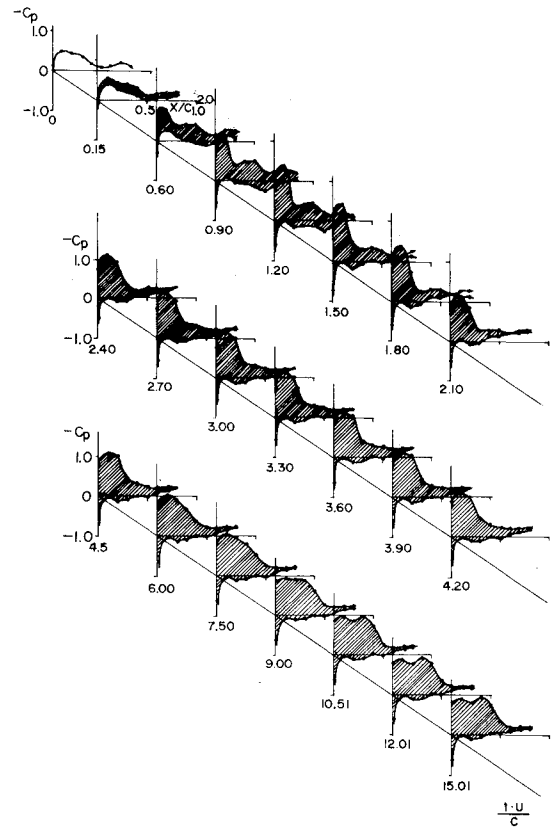

Fig. 5 Pressure distributions. $\alpha = 5.4$ deg, $T = 0.84$.

C_D is maximum at $C_{L\max}$ and, after assuming a value slightly lower than the static value at $C_{L\min}$, it recovers the static characteristic. C_m is negative maximum at $C_{L\max}$, it tends to exhibit lower stability at $C_{L\min}$, thereafter it recovers the static characteristic; but as T becomes shorter, it switches temporarily to a nose-up characteristic under conditions c and d.

$C_{L\min}$ and the corresponding transient aerodynamic characteristics are such that even within a small range of angles of attack, a temporary stall and instability will be caused by a sudden change in the angle of attack. The distribution of the static pressure coefficients C_p on the airfoil surface in Fig. 4d changes with time, as illustrated in Fig. 5. Just after the start, a strong suction near the leading edge in the upper surface and a distributed suction at midportion are observed, bringing about $C_{L\max}$ ($tU/c = 0.9 \sim 1.2$). It is seen that the subsequent stall is a result of C_p reversal in the rear part of the airfoil ($tU/c = 1.8 \sim 2.1$). Thus we have $C_p > 0$ on the upper surface, due to the formation of a vortex near the trailing edge, a flow along the lower surface is drawn out to blow down on the upper surface (flow visualization in Fig. 12a, described later). It would be easily understood that this C_p distribution generates a nose-up moment as indicated in Fig. 4. After recovery of the static characteristic at $tU/c = 3.0$, the three dynamic loads remain unchanged, even though the C_p distribution may change somewhat. C_L, C_D, and C_m are approximately constant. Some variations in the aerodynamic loading and changes in C_p distribution observed hereafter are supposedly attributable to the flowfield not being fully restored to the steady state ($tU/c = 3.0$ corresponds to 0.1 s in

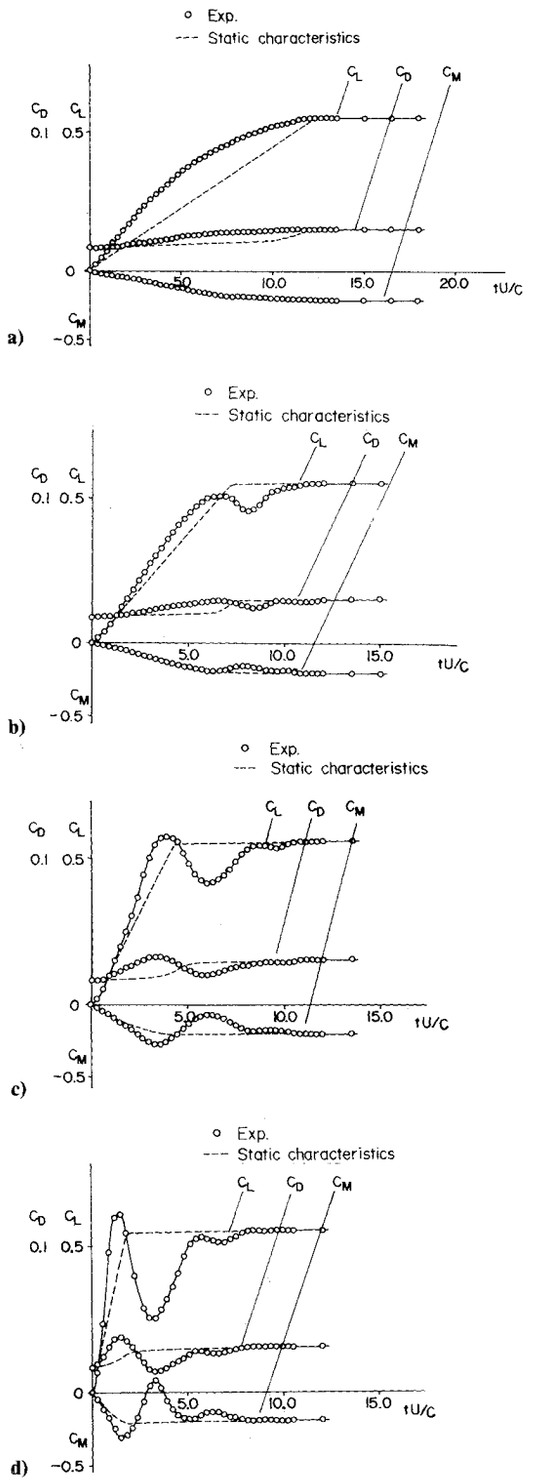

Fig. 6 Dynamic airloads on the airfoil. $\alpha = 9.0$ deg. a) $T = 12.7$, b) $T = 7.35$, c) $T = 4.5$, and d) $T = 1.90$.

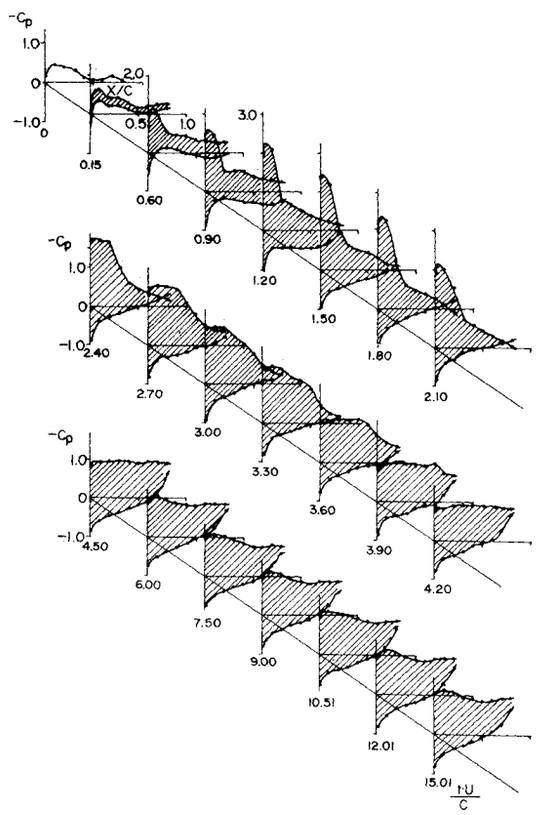

Fig. 7 Pressure distributions. $\alpha = 9.0$ deg, $T = 1.90$.

real time) or to some boundary-layer separation even in the steady state.

Generation of high $C_{L\max}$ attendant on this short stepwise change of T, stall upon release of vortex, and the process of approach to the static value from $C_{L\min}$ agree in tendency with the prediction of an analysis based on the potential theory. Namely, it is a combination of an impulsive lift at $tU/c = 0$ when T is small and a lift that gradually grows from half of the ultimate value in the linear theory, the latter being called a Wagner function. Under the conditions of the present experiment, nonlinear effects and the viscosity effects seem to be significant. The agreement in the tendency mentioned above seems to match the fact that even in a nonlinear problem the fundamental nature of the Wagner function does not change.[14]

$\alpha = 9.0$ deg

When the airfoil is raised up to a value of α a little lower than α_s, the tendency of $C_{L\max}$ and $C_{L\min}$ emerging as T becomes shorter is the same as in the case of a small angle of attack (Fig. 6); subsequent changes in characteristics are also in the same tendency. However, it is perceived that when recovery to the static characteristic from $C_{L\min}$ is made, C_L assumes a rather high value, but it tends to oscillate. As pointed out in Sec. II, this oscillation is not a mechanical but an aerodynamic one, which can be presumed from the C_p distribution, as described below. Examining the C_p distribution in Fig. 7, the aerodynamic characteristics seem to be such that, even in the range of α which does not cause a stall statically, a temporary separation of the boundary layer takes place dynamically. This incipient separation is supposedly due to an adverse pressure gradient on the wing surface caused by a strong suction developing near the leading edge in the transient state. Such a flow change naturally causes an increase of τ.

$\alpha = 30.6$ deg

It is seen (Fig. 8) that when the airfoil is raised to a large angle of attack, i.e., a higher value of α than α_s, the three dynamic loads will be quasisteady if T is long; but with a shortening of T, they will deviate far from the static values. The phenomena when T is short may substantially be regarded as a combination of the behavior from $C_{L\max}$ to $C_{L\min}$ as revealed under $\alpha = 5.4$ deg, with the effect, newly recognized under $\alpha = 9.0$ deg, of boundary-layer hysteresis. As a matter of fact, examination of the temporal change of the C_p distribution in Fig. 8d, referring to Fig. 9, indicates that at

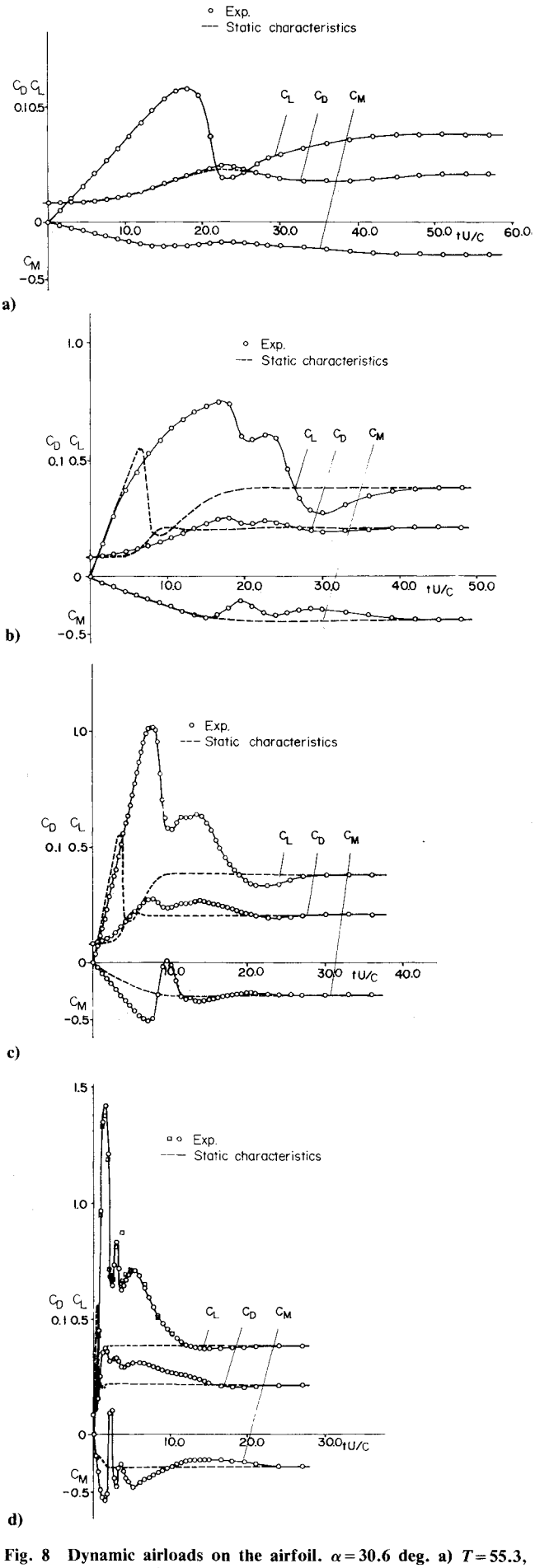

Fig. 8 Dynamic airloads on the airfoil. $\alpha = 30.6$ deg. a) $T = 55.3$, b) $T = 20.2$, c) $T = 10.1$, and d) $T = 2.01$.

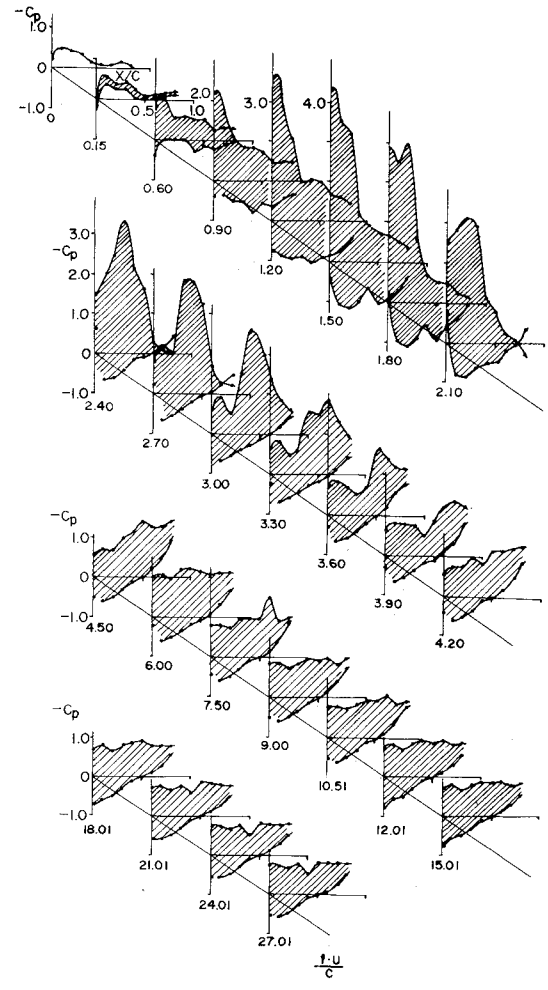

Fig. 9 Pressure distributions. $\alpha = 30.6$ deg, $T = 2.01$.

$tU/c = 1.5 \sim 1.8$ at which $C_{L\max}$ is obtained, the suction in the vicinity of the leading edge predominates, while at $tU/c = 2.1$, at which $C_{L\min}$ is obtained, a lift reversal is recognized near the trailing edge. When the vortex developed at the trailing edge flows away, the peak of the suction moves to the midportion and when C_L is best restored ($tU/c = 3.0$) the suction distribution will have two peaks, that is, near the leading edge and at the midportion. Then the central suction weakens and C_L diminishes ($tU/c = 3.3$), but as the suction at the leading edge increases and gradually moves downward ($tU/c = 3.9 \sim 4.5$), C_L again recovers. Thereafter the C_p distribution comes to exhibit a near-perfect separation on the upper surface, with C_L coming closer to the static characteristic. C_D assumes transiently a high value. C_m generates a nose-up moment at $C_{L\min}$ but thereafter changes with the C_p distribution, thereby approaching the static characteristic. Following such a complicated process, τ makes a further increase.

Thus it is understood that the transient aerodynamic characteristics depend on the transient distribution of C_p. Therefore discussion will proceed to the relation between the C_p distribution and the ambient flowfield.

From the discussions made thus for, it follows that the flow which causes a transient high C_L can be split into a portion represented by the behavior $C_{L\max} \sim C_{L\min}$ just after the start and a succeeding portion with long τ. Then in Fig. 10 are shown $(tU/c)C_{L\max}$, i.e., nondimensional time for start to attainment of $C_{L\max}$ and $(tU/c)C_{L\min}$, i.e., similar time to attainment of $C_{L\min}$ against T. It is seen that regardless of the magnitude of the static stall angle α_s, the two are functions of T. This suggests that for a certain period after the motion is started, the flow attaches to the airfoil surface regardless of

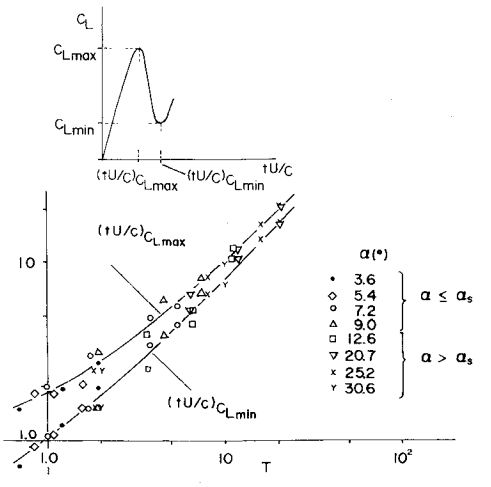

Fig. 10 Nondimensional time from start to attainment of C_{Lmax}, $(tU/c)_{C_{Lmax}}$, and of C_{Lmin}, $(tU/c)_{C_{Lmin}}$, vs nondimensional rise time T.

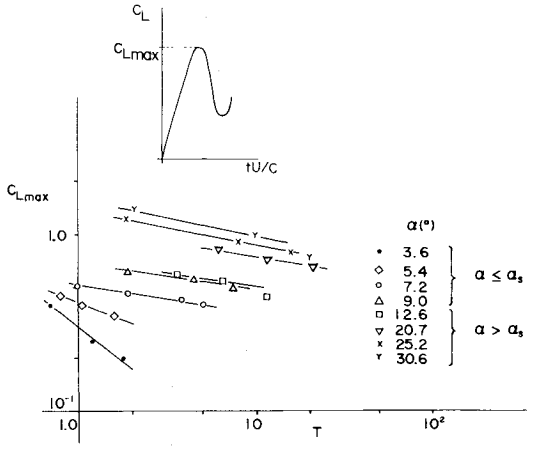

Fig. 11 C_{Lmax} just after the start vs nondimensional rise time T.

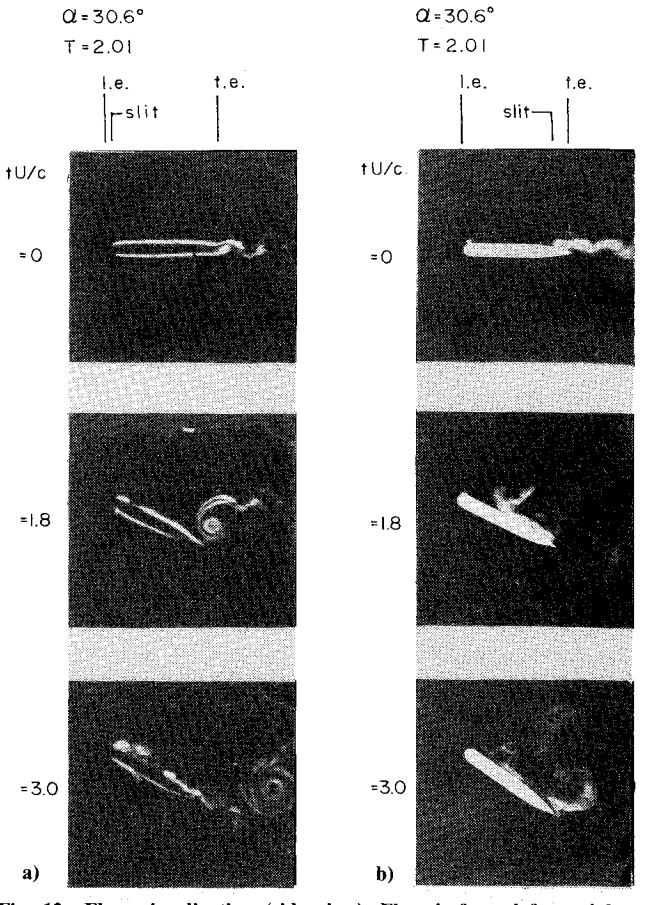

Fig. 12 Flow visualization (side view). Flow is from left to right. Vapor is issued a) near the leading edge and b) near the trailing edge. $\alpha = 30.6$ deg, $T = 2.01$.

the angle of attack, thereby generating a high lift; and an associated stall follows under the effect of a vortex shed from the trailing edge. These phenomena are likely to be closely associated with similar observations[9,10] about the oscillating airfoil. The behaviors of the first portion exhibit the same tendency as in the above-mentioned potential theory, though the magnitude of C_L or the time for vortex formation is naturally affected by viscosity. Figure 11 illustrates a change of C_{Lmax} with T. The smaller the values of α and T, the more evident is the tendency that C_{Lmax} is proportional to T^{-1}. This does not conflict with the potential theory according to which the apparent mass effect is important on C_L and C_L is proportional to the rate of change in α. Approximating the change in the angle of attack by $\alpha\{1-\cos(\pi Ut/cT)\}/2 \quad (0 \le Ut/c \le T)$, $\pi/2T$ is a reduced frequency of the oscillating airfoil; accordingly using T^{-1} instead of T in Figs. 10 and 11, the results will be comparable to the results[5-12] about the oscillating airfoil. This is, however, out of the scope of the present work. Figure 12a shows an observation of the flow around the airfoil as illustrated in Fig. 8d; it is seen that a vortex is formed at the trailing edge over the period $tU/c = 0 \sim 2.4$ and how the vortex begins to move downstream.

As for the second portion, it should be noted in the state of the lift being restored from C_{Lmin} $(tU/c = 2.4 \sim 3.0)$ shown in Figs. 8d, 9, and 12a that the maximum suction develops at the center of the wing and it is responsible for the lift; and that the ambient flow attaches to the airfoil surface but the thickness of the boundary layer periodically fluctuates in the flow direction. From Fig. 9 it is surmised that the distribution of the suction initially having a peak near the leading edge does not simply level out diffusively, but the center of the distribution shifts with a sort of flowfield induced therein. Observation of the flow above the upper surface of the airfoil, as shown in Figs. 13a and 13b, reveals that the vapor continuously flowing over the airfoil surface at $\alpha = 0$ exhibits after the start a pattern that is continuous in the span direction but periodic in the stream direction. Putting together this observation and the observation shown in Fig. 12a, it may be presumed that a two-dimensional disturbance with a periodicity in the stream direction develops transiently in the boundary layer of the upper surface and that this is intimately related to the recovery of lift recognized in Figs. 8d and 9. Based on these findings, a process as illustrated in Fig. 14 can be conceived. Namely, when a strong suction is caused impulsively and the flow is attaching to the surface, only the flow in the immediate vicinity of the wall can be reversed (Figs. 12b and 13c). As for Fig. 12b, the reversed flow was invisible from the side, and the photographs were taken from above. Therefore the thickness of the vapor is not to scale. It has been found experimentally[5] that an oscillating airfoil under high C_L condition has a transient reversed flow. It can be inferred under such a reversal of velocity that a two-dimensional vortex layer with concentrated vorticity will be generated due to a Kelvin-Helmholtz type of instability (Fig. 14b). By supposing such a mechanism, a rearward shift of a strong suction initially located near the leading edge can be explained. It seems that τ for an airfoil with a large angle of attack, depends on the period of such a vortex layer along the surface and the subsequent period of a vortex shedding from the leading edge and moving over the surface.

The preceding findings are experimental, and it should be noted that numerical analyses using Navier-Stokes equations are yielding successful results.[2] The present authors are now

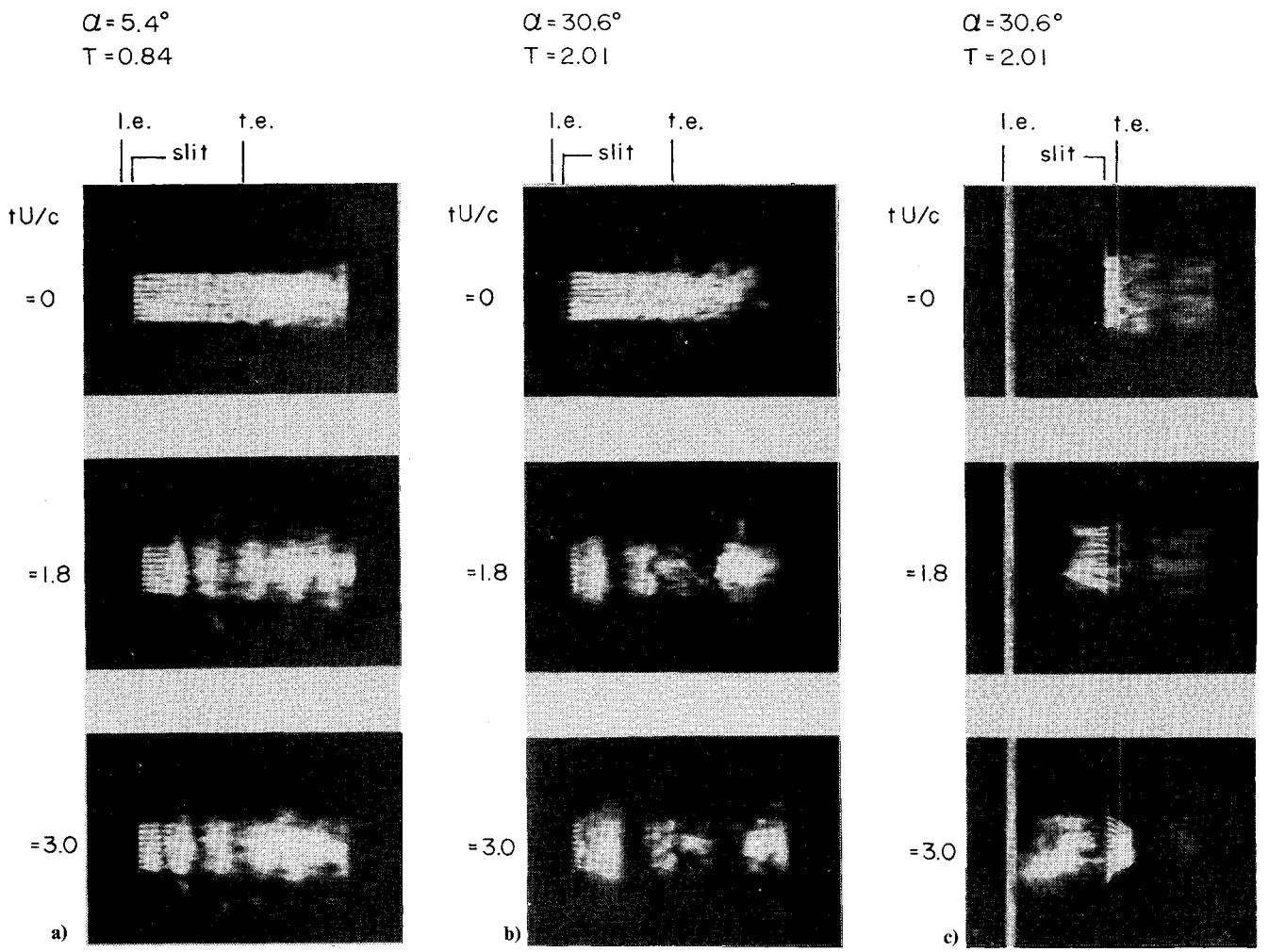

Fig. 13 Flow visualization (plan view). Flow is from left to right. Vapor is issued near the leading edge a) $\alpha = 5.4$ deg, $T = 0.84$, and b) $\alpha = 30.6$ deg, $T = 2.01$; and near the trailing edge c) $\alpha = 30.6$ deg, $T = 2.01$.

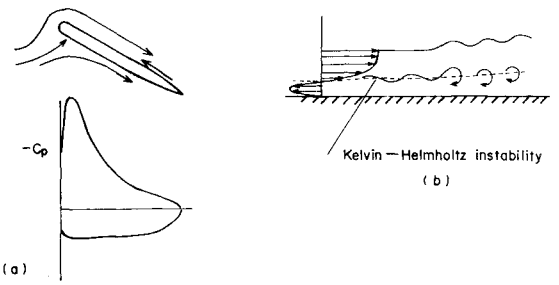

Fig. 14 Generation of vortex layer along the surface at a high angle of attack. a) Transient flow and C_p at a high angle of attack. b) Vortex layer due to Kelvin-Helmholtz instability.

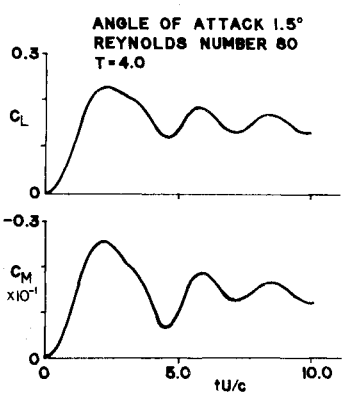

Fig. 15 Dynamic airloads on a flat plate airfoil obtained by numerical analysis. $Re = 80$, $\alpha = 1.5$ deg, $T = 4.0$.

making use of the Navier-Stokes equations and the finite element method for numerical simulations. The values of the angle of attack and Reynolds number are set lower than those in the experimental conditions. Therefore the results are not yet comparable directly with the experiments, but qualitatively there is agreement between them with respect to the transient aerodynamic characteristics (Fig. 15), streamline, and vorticity distribution. In the future, comparison between numerical analysis and experiment will certainly contribute to elucidation of this complicated, intriguing phenomenon. Generation of an intensive vortex layer over the airfoil surface will make an interesting subject of future research.

IV. Conclusions

The results of testing in which the angle of attack of a two-dimensional symmetric airfoil was increased impulsively at a Reynolds number of 2×10^4 lead to the following conclusions:

1) As the rise time T becomes shorter, the transient aerodynamic characteristics come to deviate from quasi-steadiness. When the ultimate angle of attack is sufficiently smaller than the static stall angle, first the lift becomes higher than the static value and then a sudden stalling occurs. At the time of stalling, a nose-up pitching moment develops and the airfoil exhibits an unstable characteristic. This behavior corresponds to the Wagner function in the potential theory.

When the ultimate angle of attack is close to the static stall angle or it exceeds the latter, the above-mentioned behavior is followed by generation of a lift higher than the static value and the time delay before attainment of the static characteristic becomes remarkable.

2) The phenomena of high lift generation and sudden stalling, which happen even at a small angle of attack, are caused by generation of a strong suction near the leading edge and by formation and release of a vortex near the trailing edge. The phenomena of generation and maintenance of high lift which happen at a large angle of attack are considered to be caused by formation of a vortex layer on the airfoil surface due to a steep adverse pressure gradient, as well as by movement along the surface of a vortex shedding from the leading edge.

3) A preliminary numerical analysis using the Navier-Stokes equations has yielded results which qualitatively agree with experimentation. A better understanding of the phenomenon will be achieved through the collation between further experiments and analyses.

References

[1]Orlik-Rückemann, K. J., "Aerodynamic Aspects of Aircraft Dynamics at High Angles of Attack," *Journal of Aircraft*, Vol. 20, Sept. 1983, pp. 737-752.

[2]"Unsteady Aerodynamics," *AGARD FDP Symposium*, Ottawa, Canada, AGARD-CP-227, Sept. 1977.

[3]Ham, N. D. and Garelick, M. S., "Dynamic Stall Considerations in Helicopter Rotors," *Journal of the American Helicopter Society*, Vol. 13, No. 2, 1968, pp. 49-51.

[4]Ericsson, L. E. and Reding, J. P., "Dynamic Stall of Helicopter Blades," *Journal of the American Helicopter Society*, Vol. 17, No. 1, 1972, pp. 11-19.

[5]Carr, L. W., McAlister, K. W., and McCroskey, W. J., "Analysis of the Development of Dynamic Stall Based on Oscillating Airfoil Experiments," NASA TN D-8382, 1977.

[6]McCroskey, W. J., McAlister, K. W., Carr, L. W., Pacci, S. L., Lambert, O., and Indergrand, R. F., "Dynamic Stall on Advanced Airfoil Sections," *Journal of the American Helicopter Society*, Vol. 26, No. 3, 1981, pp. 40-50.

[7]Carta, F. O., "A Comparison of the Pitching and Plunging Response of an Oscillating Airfoil," NASA CR-3172, Oct. 1979.

[8]Liiva, J., Davenport, F., Gray, L., and Walton, I., "Two-Dimensional Tests of Airfoils Oscillating near Stall," *Journal of the American Helicopter Society*, Vol. 14, No. 2, 1969, pp. 26-33.

[9]Maresca, C., Favier, D., and Rebont, J., "Unsteady Aerodynamics of an Airfoil at High Angle of Incidence Performing Various Linear Oscillations in a Uniform Stream," *Journal of the American Helicopter Society*, Vol. 26, No. 2, 1981, pp. 40-45.

[10]Favier, D., Maresca, C., and Rebont, J., "Dynamic Stall Due to Fluctuations of Velocity and Incidence," *AIAA Journal*, Vol. 20, July 1982, pp. 865-871.

[11]Ericsson, L. E. and Reding, J. P., "Dynamic Stall at High Frequency and Large Amplitude," *Journal of Aircraft*, Vol. 17, March 1980, pp. 136-142.

[12]Ericsson, L. E. and Reding, J. P., "Unsteady Flow Concepts for Dynamic Stall Analysis," *Journal of Aircraft*, Vol. 21, Aug. 1984, pp. 601-606.

[13]McCroskey, W. J., "Unsteady Airfoils," *Annual Review of Fluid Mechanics*, Vol. 14, 1982, pp. 285-311.

[14]Giesing, J. P., "Nonlinear Two-Dimensional Unsteady Potential Flow with Lift," *Journal of Aircraft*, Vol. 5, Feb. 1968, pp. 135-143.